



## Structural and electrical transport properties of Cu-doped $\text{Fe}_{1-x}\text{Cu}_x\text{Se}$ single crystals

He Li(李贺)<sup>1,2</sup>, Ming-Wei Ma(马明伟)<sup>2,3,\*</sup>, Shao-Bo Liu(刘少博)<sup>2,4</sup>, Fang Zhou(周放)<sup>2,3,4</sup>, and Xiao-Li Dong(董晓莉)<sup>2,3,4</sup>

**Citation:** Chin. Phys. B, 2020, 29 (12): 127404. DOI: 10.1088/1674-1056/abc3af

Journal homepage: <http://cpb.iphy.ac.cn>; <http://iopscience.iop.org/cpb>

### What follows is a list of articles you may be interested in

---

## Robust two-gap strong coupling superconductivity associated with low-lying phonon

### modes in pressurized $\text{Nb}_5\text{Ir}_3\text{O}$ superconductors

Bosen Wang(王铂森), Yaoqing Zhang(张尧卿), Shuxiang Xu(徐淑香), Kento Ishigaki, Kazuyuki Matsubayashi, Jin-Guang Cheng(程金光), Hideo Hosono, Yoshiya Uwatoko

Chin. Phys. B, 2019, 28 (10): 107401. DOI: 10.1088/1674-1056/ab4047

## Crystal structures and sign reversal Hall resistivities in iron-based superconductors

### $\text{Li}_x(\text{C}_3\text{H}_{10}\text{N}_2)_{0.32}\text{FeSe}$ ( $0.15 < x < 0.4$ )

Rui-Jin Sun(孙瑞锦), Shi-Feng Jin(金士锋), Jun Deng(邓俊), Mu-Nan Hao(郝木难), Lin-Lin Zhao(赵琳琳), Xiao Fan(范晓), Xiao-Ning Sun(孙晓宁), Jian-Gang Guo(郭建刚), Lin Gu(谷林)

Chin. Phys. B, 2019, 28 (6): 067401. DOI: 10.1088/1674-1056/28/6/067401

## Tunable superconductivity in parent cuprate $\text{Pr}_2\text{CuO}_{4\pm\delta}$ thin films

Xinjian Wei(魏鑫健), Ge He(何格), Wei Hu(胡卫), Xu Zhang(张旭), Mingyang Qin(秦明阳), Jie Yuan(袁洁), Beiyi Zhu(朱北沂), Yuan Lin(林媛), Kui Jin(金魁)

Chin. Phys. B, 2019, 28 (5): 057401. DOI: 10.1088/1674-1056/28/5/057401

## Observation of selective surface element substitution in $\text{FeTe}_{0.5}\text{Se}_{0.5}$ superconductor thin

### film exposed to ambient air by synchrotron radiation spectroscopy

Nian Zhang(张念), Chen Liu(刘晨), Jia-Li Zhao(赵佳丽), Tao Lei(雷涛), Jia-Ou Wang(王嘉鸥), Hai-Jie Qian(钱海杰), Rui Wu(吴蕊), Lei Yan(颜雷), Hai-Zhong Guo(郭海中), Kurash Ibrahim(奎热西)

Chin. Phys. B, 2016, 25 (9): 097402. DOI: 10.1088/1674-1056/25/9/097402

## Photoemission study of iron-based superconductor

Liu Zhong-Hao, Cai Yi-Peng, Zhao Yan-Ge, Jia Lei-Lei, Wang Shan-Cai

Chin. Phys. B, 2013, 22 (8): 087406. DOI: 10.1088/1674-1056/22/8/087406

---

# Structural and electrical transport properties of Cu-doped $\text{Fe}_{1-x}\text{Cu}_x\text{Se}$ single crystals\*

He Li(李贺)<sup>1,2</sup>, Ming-Wei Ma(马明伟)<sup>2,3,†</sup>, Shao-Bo Liu(刘少博)<sup>2,4</sup>,  
Fang Zhou(周放)<sup>2,3,4</sup>, and Xiao-Li Dong(董晓莉)<sup>2,3,4</sup>

<sup>1</sup>International Laboratory for Quantum Functional Materials of Henan, and School of Physics and Microelectronics, Zhengzhou University, Zhengzhou 450001, China

<sup>2</sup>Beijing National Laboratory for Condensed Matter Physics, Institute of Physics, Chinese Academy of Sciences, Beijing 100190, China

<sup>3</sup>Songshan Lake Materials Laboratory, Dongguan 523808, China

<sup>4</sup>University of Chinese Academy of Sciences, Beijing 100049, China

(Received 4 August 2020; revised manuscript received 22 September 2020; accepted manuscript online 22 October 2020)

We report the structural and electrical transport properties of  $\text{Fe}_{1-x}\text{Cu}_x\text{Se}$  ( $x = 0, 0.02, 0.05, 0.10$ ) single crystals grown by a chemical vapor transport method. Substituting Cu for Fe suppresses both the nematicity and superconductivity of FeSe single crystal, and provokes a metal–insulator transition. Our Hall measurements show that the Cu substitution also changes an electron dominance at low temperature of un-doped FeSe to a hole dominance of Cu-doped  $\text{Fe}_{1-x}\text{Cu}_x\text{Se}$  at  $x = 0.02$  and  $0.1$ , and reduces the sign-change temperature ( $T_R$ ) of the Hall coefficient ( $R_H$ ).

**Keywords:** iron-based superconductivity, crystal growth, element substitution, Hall coefficient

**PACS:** 74.25.F-, 74.62.Dh, 81.10.Bk, 74.70.-b

**DOI:** 10.1088/1674-1056/abc3af

## 1. Introduction

The structurally simplest FeSe exhibits distinctive normal-state properties among the iron-based superconductors and is therefore important for investigating the underlying physics of the superconductivity.<sup>[1]</sup> Its superconducting transition temperature  $T_C = 8$  K at ambient pressure,<sup>[2]</sup> which can be raised to 37 K by high pressure of 8 GPa,<sup>[3]</sup> to  $\sim 40$  K by alkali-metal<sup>[4–7]</sup> or small molecule intercalation,<sup>[8,9]</sup> and even above 65 K in one-unit-cell film on  $\text{SrTiO}_3$ .<sup>[10]</sup> FeSe undergoes a nematic transition at  $T_s = 90$  K which is rapidly suppressed by pressure and can be tuned continuously by isoelectronic S or Te substitution at Se site of FeSe.<sup>[11–13]</sup> Furthermore, with increasing pressure, the low- $T_C$  superconducting phase transforms into the high- $T_C$  phase, where the normal-state Hall resistivity changes sign from negative to positive, demonstrating a hole dominance in contrast to other FeSe-derived high- $T_C$  systems.<sup>[14]</sup> Recently, the observation of non-Fermi liquid property in  $\text{FeSe}_{1-x}\text{S}_x$  and the topological nature of  $\text{FeSe}_{1-x}\text{Te}_x$  have triggered renewed interest.<sup>[15,16]</sup> Besides isoelectronic S and Te substitution at Se site, transition elements substitution at Fe site of FeSe would be also of interest for their comparable ionic sizes to Fe and the potential to tune the carrier type and concentration or investigate magnetic or non-magnetic impurity effect on superconductivity.<sup>[17–24]</sup>

Earlier studies of Cu-substituted FeSe powder samples show that Cu substitution at Fe site in FeSe suppresses superconductivity and provokes a metal–insulator transition.<sup>[21,22]</sup>

Under a relatively small pressure of 1.5 GPa, superconductivity in  $\text{Cu}_{0.04}\text{Fe}_{0.97}\text{Se}$  is restored below 6.6 K; and  $T_C$  is increased to its maximum of 31.3 K upon an applied pressure at 7.8 GPa.<sup>[23]</sup> Detailed Mössbauer spectroscopy studies on the  $^{57}\text{Fe}$ -enriched  $\text{Cu}_{0.04}\text{Fe}_{0.97}\text{Se}$  powder sample reveal that part of the iron sites are magnetically ordered at low temperature, and the static magnetic moments destroy the superconducting pairing. Raising pressure leads to a collapse of the static magnetism and restoration of superconductivity with the maximal  $T_C$  value at 8 GPa.<sup>[24]</sup> In contrast to the extensive studies on the intrinsic properties of isoelectronically substituted  $\text{FeSe}_{1-x}\text{S}_x$  and  $\text{FeSe}_{1-x}\text{Te}_x$  due to the availability of high-quality single crystals,<sup>[1]</sup> few study of transition elements substitution effect is reported in FeSe single crystals. In the present paper, we report the structural and electrical transport properties of  $\text{Fe}_{1-x}\text{Cu}_x\text{Se}$  ( $x = 0–0.10$ ) single crystals. Cu substitution suppresses both the nematicity and superconductivity of the FeSe single crystal, provokes a metal–insulator transition, changes an electron dominance at low temperature of un-doped FeSe to a hole dominance of Cu-doped  $\text{Fe}_{1-x}\text{Cu}_x\text{Se}$  at  $x = 0.02$  and  $0.1$ , and reduces the sign-change temperature ( $T_R$ ) of the Hall coefficient ( $R_H$ ).

## 2. Experiments

A series of  $\text{Fe}_{1-x}\text{Cu}_x\text{Se}$  ( $x = 0, 0.02, 0.05, 0.10$ ) single crystals were grown by a chemical vapor transport method, us-

\*Project supported by the National Key Research and Development of China (Grant No. 2018YFA0704200), the National Natural Science Foundation of China (Grant No. 11834016), and the Strategic Priority Research Program of Chinese Academy of Sciences (Grant No. XDB25000000).

†Corresponding author. E-mail: [mw\\_ma@iphy.ac.cn](mailto:mw_ma@iphy.ac.cn)

ing high-purity Fe, Cu, Se powders as raw materials and mixture of  $\text{AlCl}_3$  and  $\text{KCl}$  as transport agent.<sup>[25]</sup> The temperature of the hot and cold positions was kept at  $400^\circ\text{C}$  and  $350^\circ\text{C}$ , respectively. After a duration of 30 days, single crystals with a size of 3–5 mm were grown around the cold part of the quartz tube. The experimental details are given in Table 1.

**Table 1.** Experimental details for growing  $\text{Fe}_{1-x}\text{Cu}_x\text{Se}$  single crystals.

Nominal composition	Transport agent mole ratio	$T_{\text{hot}} - T_{\text{cold}}$	Actual composition
$\text{FeSe}_{0.94}$	$\text{AlCl}_3:\text{KCl} = 3:1$	$400^\circ\text{C} - 350^\circ\text{C}$	$\text{FeSe}$
$\text{Fe}_{0.95}\text{Cu}_{0.05}\text{Se}_{0.94}$	$\text{AlCl}_3:\text{KCl} = 3:1$	$400^\circ\text{C} - 350^\circ\text{C}$	$\text{Fe}_{0.98}\text{Cu}_{0.02}\text{Se}$
$\text{Fe}_{0.9}\text{Cu}_{0.1}\text{Se}_{0.94}$	$\text{AlCl}_3:\text{KCl} = 3:1$	$400^\circ\text{C} - 350^\circ\text{C}$	$\text{Fe}_{0.95}\text{Cu}_{0.05}\text{Se}$
$\text{Fe}_{0.8}\text{Cu}_{0.2}\text{Se}_{0.94}$	$\text{AlCl}_3:\text{KCl} = 3:1$	$400^\circ\text{C} - 350^\circ\text{C}$	$\text{Fe}_{0.9}\text{Cu}_{0.1}\text{Se}$

The actual chemical composition of  $\text{Fe}_{1-x}\text{Cu}_x\text{Se}$  single crystals was determined by inductively coupled plasma atomic emission spectroscopy. The x-ray diffraction (XRD) measurements were performed on the x-ray diffractometer (MXP18A-HF) used copper  $K_\alpha$  radiation. Electrical transport measure-

ments up to 9 T were performed on a Quantum Design PPMS-9 system.

### 3. Results and discussion

The results of powder XRD at room temperature demonstrate that the  $\text{Fe}_{1-x}\text{Cu}_x\text{Se}$  single crystals are of single phase and all the diffraction peaks can be well indexed with a previously reported tetragonal structure,<sup>[21,22]</sup> as shown in Fig. 1(a). Figure 1(b) shows the single crystal XRD patterns for all the  $\text{Fe}_{1-x}\text{Cu}_x\text{Se}$  ( $x = 0, 0.02, 0.05, 0.10$ ) single crystals. Only (0 0  $l$ ) reflections are observed, indicating that the single crystals are in perfect (0 0 1) orientation. Figure 1(c) shows the lattice parameters  $a$  and  $c$  as functions of the Cu doping level. With increasing Cu content, the lattice parameter  $a$  increases monotonically, while  $c$  decreases monotonically, consistent with previous reports.<sup>[21,22]</sup> As displayed in Fig. 1(d), the unit cell volume  $V = a^2c$  increases linearly with increasing Cu content.

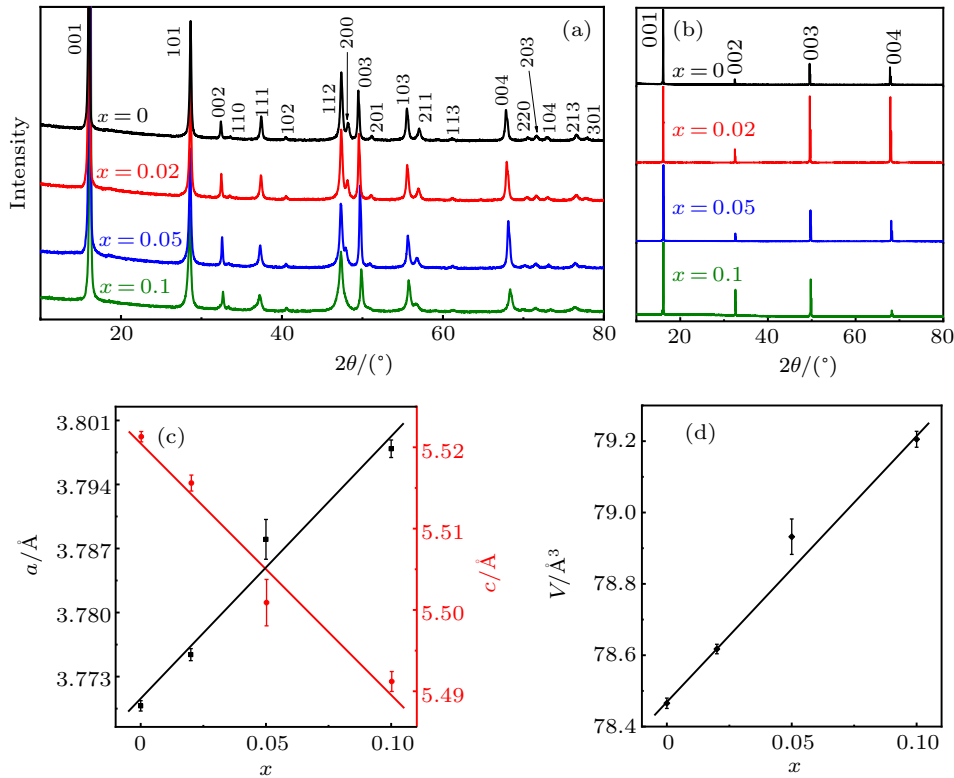


**Fig. 1.** (a) Powder XRD patterns for  $\text{Fe}_{1-x}\text{Cu}_x\text{Se}$ . (b) Single crystal XRD for  $\text{Fe}_{1-x}\text{Cu}_x\text{Se}$ . (c) Variation of refined lattice parameters  $a$  and  $c$  with Cu doping level  $x$ . (d) Variation of unit cell volume  $V = a^2c$  with Cu doping level  $x$ .

Figure 2 shows the temperature dependence of the normalized electrical resistivity  $\rho(T)/\rho(300\text{ K})$  and specific heat measured for  $\text{Fe}_{1-x}\text{Cu}_x\text{Se}$  ( $x = 0, 0.02, 0.05, 0.10$ ) single crystals. Pure FeSe is superconducting at  $T_C = 8.3\text{ K}$  and the kink at  $T_s = 90\text{ K}$  in the resistivity curve represents the nematic transition, which is more clearly visible from a dip in the temperature derivative of the resistivity as shown in the inset of Fig. 2(a) and a jump in the specific heat as displayed in Fig. 2(b). A small Cu doping of 2% can completely sup-

press the superconductivity and nematicity, as no such kink and jump can be found in the resistivity and specific heat measurements, respectively [Figs. 2(a) and 2(b)]. While the resistivity of FeSe in the normal state demonstrates a metallic behavior, an upturn with decreasing temperature appears around 42 K in the resistivity of  $\text{Fe}_{0.98}\text{Cu}_{0.02}\text{Se}$ , indicating a transition behavior from metallic to semiconducting with Cu doping. At Cu doping level  $x = 0.05$  and  $0.10$ , the resistivity increases quickly with cooling, showing an insulating behavior in the

whole temperature range, which is in agreement with previous results of powder sample. The metal-insulator transition in  $\text{Fe}_{1-x}\text{Cu}_x\text{Se}$  can be probably attributed to Anderson localization arising from disorder.<sup>[26,27]</sup>

To further investigate the effects of Cu doping on the electrical transport properties, we measured the Hall effect of  $\text{Fe}_{1-x}\text{Cu}_x\text{Se}$  ( $x = 0, 0.02, 0.05, 0.10$ ) single crystals. Figure 3 shows the Hall resistivity  $\rho_{xy}$  at various temperatures with different Cu doping level. As seen in Fig. 3(a),  $\rho_{xy}$  of stoichiometric FeSe shows a linear field dependence for  $T > 50$  K, in accordance with the compensated semimetal character, and the slope changes sign twice from positive to negative and then back to positive upon cooling.<sup>[28]</sup> A non-linearity develops for  $\rho_{xy}$  and the initial slope eventually becomes negative for  $T \leq 50$  K, but tends to change sign again under higher magnetic field. Unlike pure FeSe, the common feature of  $\rho_{xy}$  curves for  $\text{Fe}_{1-x}\text{Cu}_x\text{Se}$  with  $x = 0.02, 0.05, 0.1$  is that no non-linearity develops in the whole temperature and magnetic field range. For  $\text{Fe}_{0.98}\text{Cu}_{0.02}\text{Se}$  as shown in Fig. 3(b), the slope changes sign twice from positive to negative and then back to positive and remains positive upon cooling to 10 K. For  $\text{Fe}_{0.95}\text{Cu}_{0.05}\text{Se}$  as displayed in Fig. 3(c), the slope changes sign once from positive to negative at  $T = 140$  K. For  $\text{Fe}_{0.90}\text{Cu}_{0.10}\text{Se}$ , the slope always remains positive in the whole temperature range without any sign change as presented in Fig. 3(d).

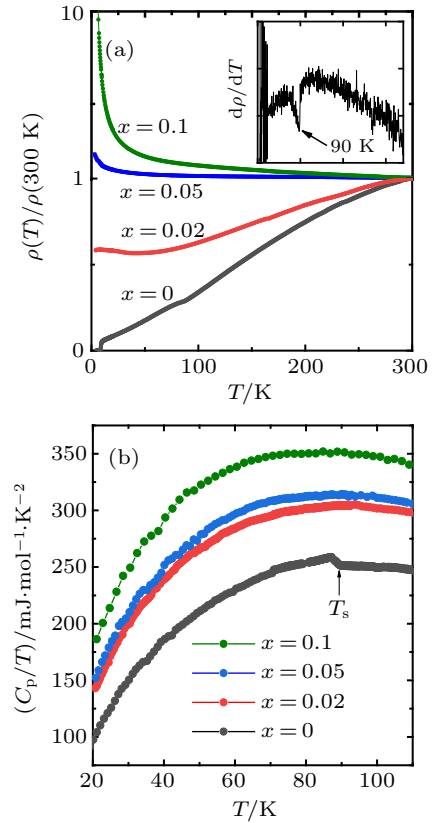


Fig. 2. (a) Temperature dependence of the normalized resistivity  $\rho(T)/\rho(300\text{ K})$  in  $\text{Fe}_{1-x}\text{Cu}_x\text{Se}$ . Inset shows the temperature dependence of the first derivative of resistivity for FeSe. (b) Specific heat measurement displayed by the  $C_p/T$  versus  $T$  plots for  $\text{Fe}_{1-x}\text{Cu}_x\text{Se}$ .

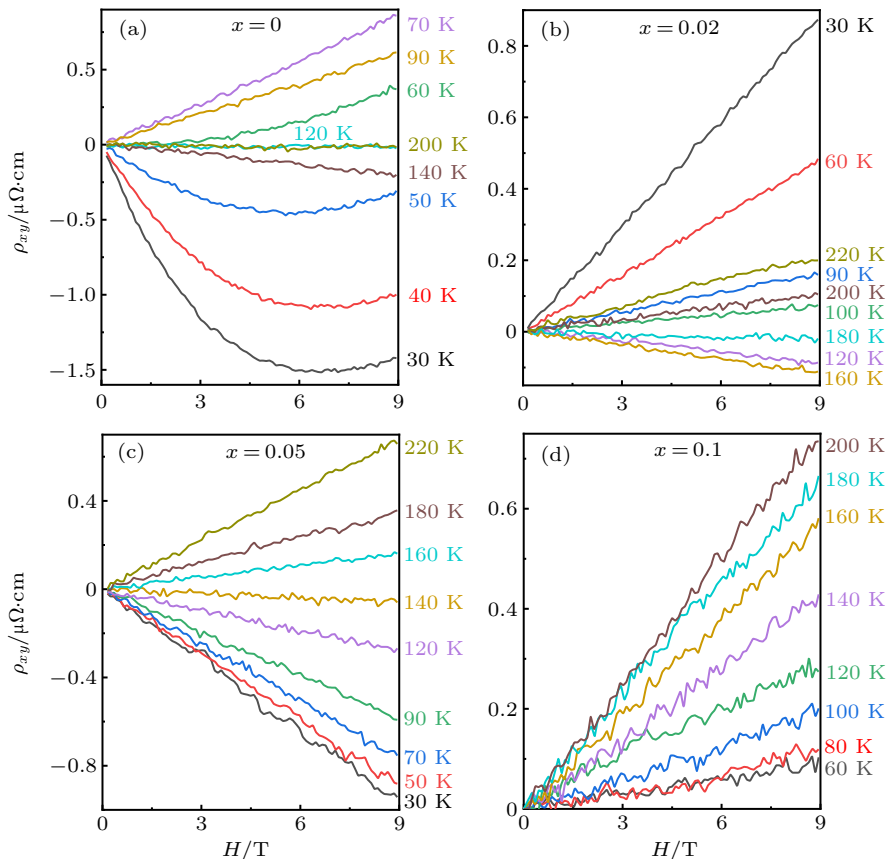
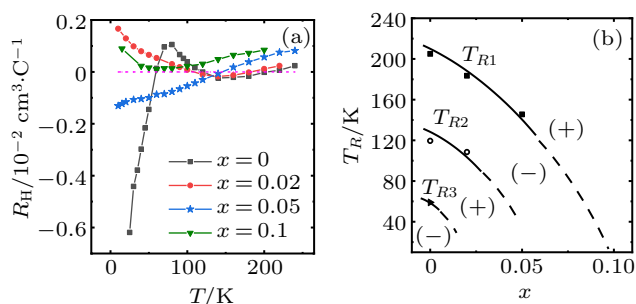


Fig. 3. Magnetic field ( $H$ ) dependence of Hall resistivity ( $\rho_{xy}$ ) of  $\text{Fe}_{1-x}\text{Cu}_x\text{Se}$  with  $x = 0$  (a), 0.02 (b), 0.05 (c), and 0.1 (d) in the temperature range from 30 K to room temperature.



**Fig. 4.** (a) Temperature dependence of Hall coefficient ( $R_H$ ) of  $\text{Fe}_{1-x}\text{Cu}_x\text{Se}$  with  $x = 0, 0.02, 0.05,$  and  $0.1$  estimated by  $R_H \equiv d\rho_{xy}/dH$ , at the zero-field limit. (b) The suppression of the sign change temperature  $T_R$  of  $R_H$  with Cu doping level  $x$ . The solid and dotted curves are guides to the eyes.

We plot in Fig. 4(a) the temperature dependence of the Hall coefficient, defined as the field derivative of  $\rho_{xy}$ ,  $R_H \equiv d\rho_{xy}/dH$ , at the zero-field limit. The sign of the Hall coefficient  $R_H$  is an indicator of the dominant carrier type. The temperature dependence of  $R_H$  is shown in Fig. 4(a). With cooling, the Hall coefficient of FeSe changes sign at three temperatures  $T_{R1}$ ,  $T_{R2}$ , and  $T_{R3}$ , from positive to negative at  $T_{R1} = 205$  K, then from negative to positive at  $T_{R2} = 120$  K with a moderate enhancement of  $R_H$  before  $T_s$ , and finally reversed again at  $T_{R3} = 59$  K, exhibiting a tendency to strongly negative values below  $T_s$ . The evolution with Cu doping of the sign-change temperature  $T_R$  of the Hall coefficient is summarized in Fig. 4(b). All the three temperatures  $T_{R1}$ ,  $T_{R2}$ , and  $T_{R3}$  are gradually reduced with Cu doping, with  $T_{R1}$  tending to vanish towards Cu doping  $x = 0.1$ , which indicates a hole dominant carrier type.

As we know, the valence state of the Fe atom in FeSe and other iron-based superconductors is assigned as  $\text{Fe}^{2+}$ , so the Fe atoms are formally in the  $3d^6$  electronic configuration. Also, electronic structure calculations for  $\text{SrCu}_2\text{As}_2$  and  $\text{BaCu}_2\text{As}_2$  predicted that the Cu atoms have a formal valence state of  $\text{Cu}^{1+}$  and a nonmagnetic and chemically inert  $3d^{10}$  electronic configuration.<sup>[29]</sup> Anand *et al.* confirmed this result by measuring the electronic and magnetic properties of  $\text{SrCu}_2\text{As}_2$  and  $\text{BaCu}_2\text{As}_2$ , suggesting that Cu substitution for Fe in  $(\text{Ca}, \text{Sr}, \text{Ba})(\text{Fe}_{1-x}\text{Cu}_x)_2\text{As}_2$  should result in hole doping.<sup>[30]</sup> We infer that Cu substitution in FeSe plays a role of hole doping which leads to the suppression of sign change temperatures  $T_{R1}$ ,  $T_{R2}$ , and  $T_{R3}$  of the Hall coefficient and hole dominant carrier type in  $\text{Fe}_{1-x}\text{Cu}_x\text{Se}$ .

#### 4. Conclusion

We have successfully grown a series of  $\text{Fe}_{1-x}\text{Cu}_x\text{Se}$  single crystals with  $x = 0, 0.02, 0.05,$  and  $0.1$ . With increasing Cu doping content, the lattice parameter  $a$  increases monotonically, while the lattice parameter  $c$  decreases monotonically. Both the resistivity and specific heat measurements indicate that Cu doping suppresses nematicity and superconductivity and provokes a metal-insulator transition in  $\text{Fe}_{1-x}\text{Cu}_x\text{Se}$ . Also, Cu substitution changes an electron dominance at low temperature of un-doped FeSe to a hole dominance of Cu-

doped  $\text{Fe}_{1-x}\text{Cu}_x\text{Se}$  at  $x = 0.02$  and  $0.1$ , and reduces the sign-change temperature ( $T_R$ ) of the Hall coefficient ( $R_H$ ).

#### References

- [1] Shibauchi T, Hanaguri T and Matsuda Y 2020 *J. Phys. Soc. Jpn.* **89** 102002
- [2] Hsu F C, Luo J Y, Yeh K W, Chen T K, Huang T W, Wu P M, Lee Y C, Huang Y L, Chu Y Y, Yan D C and Wu M K 2008 *Proc. Natl. Acad. Sci. USA* **105** 14262
- [3] Medvedev S, McQueen T M, Troyan A I, Palasyuk T, Eremets M I, Cava R J, Naghavi S, Casper F, Ksenofontov V, Wortmann G and Felser C 2009 *Nat. Mater.* **8** 630
- [4] Guo J G, Jin S F, Wang G, Wang S C, Zhu K X, Zhou T T, He M and Chen X L 2010 *Phys. Rev. B* **82** 180520(R)
- [5] Wang A F, Ying J J, Yan Y J, Liu R H, Luo X G, Li Z Y, Wang X F, Zhang M, Ye G J, Cheng P, Xiang Z J and Chen X H 2011 *Phys. Rev. B* **83** 060512(R)
- [6] Krzton-Maziopa A, Sheradini Z, Pomjakushina E, Pomjakushin V, Bendele M, Amato A, Khasanov R, Luetkens H and Conder K 2011 *J. Phys.: Condens. Matter* **23** 052203
- [7] Ying T P, Chen X L, Wang G, Jin S F, Zhou T T, Lai X F, Zhang H and Wang W Y 2012 *Sci. Rep.* **2** 426
- [8] Lu X F, Wang N Z, Wu H, Wu Y P, Zhao D, Zeng X Z, Luo X G, Wu T, Bao W, Zhang G H, Huang F Q, Huang Q Z and Chen X H 2015 *Nat. Mater.* **14** 325
- [9] Dong X L, Jin K, Yuan D N, Zhou H X, Yuan J, Huang Y L, Hua W, Sun J L, Zheng P, Hu W, Mao Y Y, Ma M W, Zhang G M, Zhou F and Zhao Z X 2015 *Phys. Rev. B* **92** 064515
- [10] He S L, He J F, Zhang W H, *et al.* 2013 *Nat. Mater.* **12** 605
- [11] Sun J P, Matsuura K, Ye G Z, Mizukami Y, Shimozawa M, Matsubayashi K, Yamashita M, Watashige T, Kasahara S, Matsuda Y, Yan J Q, Sales B C, Uwatoko Y, Cheng J G and Shibauchi T 2016 *Nat. Commun.* **7** 12146
- [12] Matsuura K, Mizukami Y, Arai Y, *et al.* 2017 *Nat. Commun.* **8** 1143
- [13] Terao K, Kashiwagi T, Shizu T, Klemm R A and Kadowaki K 2019 *Phys. Rev. B* **100** 224516
- [14] Sun J P, Ye G Z, Shahi P, Yan J Q, Matsuura K, Kontani H, Zhang G M, Zhou Q, Sales B C, Shibauchi T, Uwatoko Y, Singh D J and Cheng J G 2017 *Phys. Rev. Lett.* **118** 147004
- [15] Licciardello S, Buhot J, Lu J, Ayres J, Kasahara S, Matsuda Y, Shibauchi T and Hussey N E 2019 *Nature* **567** 213
- [16] Yin J X, Wu Z, Wang J H, Ye Z Y, Gong J, Hou X Y, Shan L, Li A, Liang X J, Wu X X, Li J, Ting C S, Wang Z Q, Hu J P, Hor P H, Ding H and Pan S H 2015 *Nat. Phys.* **11** 543
- [17] Urata T, Tanabe Y, Huynh K K, Yamakawa Y, Kontani H and Tanigaki K 2016 *Phys. Rev. B* **93** 014507
- [18] Wu M K, Hsu F C, Yeh K W, *et al.* 2009 *Physica C* **469** 340
- [19] Yadav A K, Thakur A D and Tomy C V 2011 *Solid State Commun.* **151** 557
- [20] Yadav A K, Sanchela A V, Thakur A D and Tomy C V 2015 *Solid State Commun.* **202** 8
- [21] Williams A J, McQueen T M, Ksenofontov V, Felser C and Cava R J 2009 *J. Phys.: Condens. Matter* **21** 305701
- [22] Huang T W, Chen T K, Yeh K W, Ke C T, Chen C L, Huang Y L, Hsu F C, Wu M K, Wu P M, Avdeev M and Studer A J 2010 *Phys. Rev. B* **82** 104502
- [23] Schoop L M, Medvedev S A, Ksenofontov V, Williams A, Palasyuk T, Troyan I A, Schmitt J, Casper F, Wang C H, Eremets M, Cava R J and Felser C 2011 *Phys. Rev. B* **84** 174505
- [24] Shylin S I, Ksenofontov V, Naumov P G, Medvedev S A and Felser C 2018 *J. Supercond. Nov. Magn.* **31** 763
- [25] Chareev D, Osadchii E, Kuzmicheva T, Lin J Y, Kuzmichev S, Volkova O and Vasiliev A 2013 *CrystEngComm* **15** 1989
- [26] Chadov S, Schärff D, Fecher G H and Felser C 2010 *Phys. Rev. B* **81** 104523
- [27] Young B L, Wu J, Huang T W, Yeh K W and Wu M K 2010 *Phys. Rev. B* **81** 144513
- [28] Watson M D, Yamashita T, Kasahara S, Knafo W, Nardone M, Béard J, Hardy F, McCollam A, Narayanan A, Blake S F, Wolf T, Haghghirad A A, Meingast C, Schofield A J, Löhneysen H, Matsuda Y, Coldea A I and Shibauchi T 2015 *Phys. Rev. Lett.* **115** 027006
- [29] Singh D J 2009 *Phys. Rev. B* **79** 153102
- [30] Anand V K, Perera P K, Pandey A, Goetsch R J, Kreyssig A and Johnston D C 2012 *Phys. Rev. B* **85** 214523